

Acylation-dependent Protein Export in *Leishmania**

(Received for publication, November 15, 1999, and in revised form, January 10, 2000)

Paul W. Denny‡, Suzanne Gokool§, David G. Russell¶, Mark C. Field, and Deborah F. Smith**

From the Wellcome Trust Laboratories for Molecular Parasitology, Department of Biochemistry,
Imperial College of Science, Technology and Medicine, London SW7 2AZ, United Kingdom and

¶Department of Molecular Microbiology, Washington University Medical School, St. Louis, Missouri 63110

The surface of the protozoan parasite *Leishmania* is unusual in that it consists predominantly of glycosylphosphatidylinositol-anchored glycoconjugates and proteins. Additionally, a family of hydrophilic acylated surface proteins (HASPs) has been localized to the extracellular face of the plasma membrane in infective parasite stages. These surface polypeptides lack a recognizable endoplasmic reticulum secretory signal sequence, transmembrane spanning domain, or glycosylphosphatidylinositol-anchor consensus sequence, indicating that novel mechanisms are involved in their transport and localization. Here, we show that the N-terminal domain of HASPB contains primary structural information that directs both *N*-myristoylation and palmitoylation and is essential for correct localization of the protein to the plasma membrane. Furthermore, the N-terminal 18 amino acids of HASPB, encoding the dual acylation site, are sufficient to target the heterologous *Aequorea victoria* green fluorescent protein to the cell surface of *Leishmania*. Mutagenesis of the predicted acylated residues confirms that modification by both myristate and palmitate is required for correct trafficking. These data suggest that HASPB is a representative of a novel class of proteins whose translocation onto the surface of eukaryotic cells is dependent upon a “non-classical” pathway involving *N*-myristoylation/palmitoylation. Significantly, HASPB is also translocated on to the extracellular face of the plasma membrane of transfected mammalian cells, indicating that the export signal for HASPB is recognized by a higher eukaryotic export mechanism.

Protozoan parasites of the genus *Leishmania* cause a spectrum of tropical and sub-tropical diseases termed the leishmaniasis. *Leishmania* live as either extracellular, flagellated promastigotes in the digestive tract of their sandfly vector or as aflagellated amastigotes within the phagolysosomes of mammalian macrophages (1). Much research has focused on the unusually high levels of glycosylphosphatidylinositol (GPI)¹-

anchored surface molecules present in these organisms (2), particularly the unique glycoconjugate, lipophosphoglycan (LPG), abundant in promastigotes (3), and the metalloprotease GP63 (or leishmanolysin) (4). The hydrophilic acylated surface proteins (HASPs; originally named GBP and GA/CP in *Leishmania major*) are a family of related surface molecules expressed only in infective parasite stages (5, 6). These proteins are unusual in that they lack a “classical” endoplasmic reticulum (ER) secretory signal sequence, a GPI-anchor consensus, or membrane-spanning domains but are surface-localized (6), partition into the hydrophobic phase on Triton X-114 separation, and fractionate with lipid species (5). The mechanism of transport and attachment to the cell surface is unclear, although it has been suggested that this may occur by virtue of a close association with LPG via an HASP repeat region with homology to the peptidoglycan binding domain of *Staphylococcus aureus* protein A (6). More recent studies have not substantiated this hypothesis, as HASPs are still presented on the surface of infective metacyclic parasites in the absence of LPG (7).

Leishmania (and other trypanosomatids) possess a conventional eukaryotic secretory pathway (8, 9) and require a signal sequence for translocation of secreted proteins into the ER (10). However, a number of specialized features are apparent in the secretory systems of *Leishmania* and related organisms, particularly the necessity to traffic large quantities of lipid-anchored molecules to the cell surface. In addition, and uniquely to these parasites, all exo- and endocytosis at the cell surface occurs via the flagellar pocket, an invagination of the plasma membrane at the base of the single flagellum (11, 12).

Absence of ER secretory signals within the HASP family would preclude ER transport through the classical secretory pathway, *i.e.* via translocation through a sec61p complex into the ER lumen. This suggestion is supported by the observation that HASPB is not glycosylated, despite the presence of several consensus *N*-glycosylation sites.² These properties place HASPB among a group of eukaryotic proteins that lack an ER-targeting secretory signal but are still exported out of the cell, by so called “non-classical” transport (13, 14). Examples of proteins undergoing non-classical export include fibroblast growth factors-1 and -2, interleukin-1, yeast *a*-factor, and galectin. Export of *Saccharomyces cerevisiae a*-factor is the best understood; this short, 12-amino acid lipoprotein is exported via an ATP binding cassette transporter (15). By contrast, galectin appears to be released from the plasma membrane of mammalian cells through vesicular budding (16), possibly via a novel pathway involving a transporter (17). It is unclear at

* This work was supported in part by Wellcome Trust Grant 045493/Z/95/Z/JRS/JH. The costs of publication of this article were defrayed in part by the payment of page charges. This article must therefore be hereby marked “advertisement” in accordance with 18 U.S.C. Section 1734 solely to indicate this fact.

‡ Supported by Leverhulme Trust Grant F/58/AT.

§ Current address: Max-Planck-Institut für Biologie, Abteilung Membran-biochemie, D-72076 Tübingen, Germany.

¶ Supported by United States Public Health Service Grant AI 37977 and recipient of a Burroughs Wellcome Scholar award in Molecular Parasitology.

** To whom correspondence should be addressed. Tel.: 44-207-594-5282; Fax: 44-207-594-5283; E-mail: d.smith@ic.ac.uk.

¹ The abbreviations used are: GPI, glycosylphosphatidylinositol; HASP, hydrophilic acylated surface protein; LPG, lipophosphoglycan; ER, endoplasmic reticulum; GFP, green fluorescent protein; EGFP,

enhanced GFP; conA, concanavalin A; DRM, detergent-resistant membranes; CHO, Chinese hamster ovary; BSA, bovine serum albumin; PBS, phosphate-buffered saline; DAPI, 4',6'-dianidino-2-phenylindole; Pipes, 1,4-piperazinediethanesulfonic acid; hGH, human growth hormone.

² T. M. Alce and D. F. Smith, unpublished data.

present whether the examples of “non-classically” exported proteins cited above use the same or different mechanisms, and it is highly possible that several auxiliary systems are present.

Here we report that the 18-amino acid N-terminal region of HASPB is acylated *in vivo* and is sufficient to target a heterologous protein (*Aequorea victoria* green fluorescent protein, GFP) to the cell surface of *Leishmania*. In addition, we demonstrate that HASPB is also exported by mammalian cells, suggesting that this pathway is also present in higher eukaryotes.

EXPERIMENTAL PROCEDURES

Maintenance and Manipulation of *Leishmania*—*L. major* parasites (MHOM/IL/81/Friedlin; FV1 strain) were maintained at 26 °C in Medium 199 (Life Technologies, Inc.) supplemented with 20% fetal calf serum (Life Technologies, Inc.). Transfections were performed as described previously with the *pX NEO* episome (18), and cultures were subsequently grown in media supplemented with 1 mg/ml G418 (Life Technologies, Inc.). Cells were metabolically labeled in serum-free media containing 200 μ Ci/ml [9,10-³H]myristate (53 Ci/mmol) or [9,10-³H]palmitate (52 Ci/mmol) (Amersham Pharmacia Biotech) conjugated to de-fatted BSA (Sigma) according to published protocols (19).

Maintenance and Manipulation of Mammalian Cells—CHO cells were cultured on glass coverslips using Dulbecco's modified Eagle's medium (Life Technologies, Inc.) supplemented with 10% fetal calf serum. Transfections were performed using LipofectAMINE (Life Technologies, Inc.) according to the manufacturer's protocol. Typically, 1 μ g of expression plasmid and 15 μ l of LipofectAMINE were used, and cells were allowed to recover for 24 h before study.

Construction of Gene Fusions—All procedures were performed according to manufacturers' instructions. All gene fusions were generated by polymerase chain reactions using the *Pfu* polymerase (Stratagene), purified using the QIAEX II system (Qiagen), and cloned directly into *pX NEO* unless stated otherwise. Deoxyoligonucleotide primers are shown 5' to 3' with sequence complementary to the target template in bold and restriction sites underlined.

L. major HASPB 3'-tagged with *GENE10* encoding an 11-amino acid peptide (Novagen) was generated by polymerase chain reaction using cloned HASPB as template, a 5' primer (primer 1) containing a *Bam*HI site (CGCATCTAGACATATGGATCCTATCTATCTCCCGCTTAT-ACACC), and a 3' primer (primer 2) encoding an *Xba*I site and the *GENE10* tag (CATAGATCTAGACTAGCGACCCATTGCTGTCCACCAAGTCATGCTAGCCATGTTGCCGGCAGCGTGCTCCTTC). The product was cloned into *pX NEO* to create *pX NEO HASPB::GENE10* and into the mammalian vector *pSG5* to generate *pSG5 HASPB::GENE10*. 18- and 55-amino acid N-terminal deletions of *HASPB::GENE10* were made using 3' primer 2 and 5' primers (primers 3 and 4) containing *Bam*HI sites: (CGCATCTAGACATATGGATCCTATCTATCTCCCGCTTATACACCATGAACACGAAGACCGTTGCCCGAAG), respectively. The fusions were cloned to make *pX NEO Δ 1-18haspb::GENE10* and *pX NEO Δ 1-55haspb::GENE10*.

The sequence encoding the N-terminal 18 amino acids of HASPB was amplified using 5' primer 1 and a 3' primer (primer 5) containing an *Eco*RV site (TAGAGATATCCGCACCTTTCTGGGGCTC) and cloned into pBluescript to form pBluescript *HASPB18b*. The EGFP gene (20) (kindly provided by Dr. Neil Fairweather, Imperial College) was amplified using a 5' primer (primer 6) containing an *Eco*RV site (TAGAGATATCATGAGTAAAGGAGAAGAAGCTTTTCACTGGA), and a 3' primer (primer 7) encoding a *Hind*III and an *Xba*I site (CCCAGC-TTTCTAGATTATTGTTATAGTTCATCCATGCCCAGT), and cloned into pBluescript *HASPB18b* using *Eco*RV and *Hind*III to make pBluescript *HASPB18b::GFP*. 5' primers (primers 8–11) containing *Bam*HI sites (CGCGGATCCATGG(G/C)AAGCTCTT(G/C)CACGAAGG) were designed to introduce point mutations into the 5' *HASPB* sequence. Gene fusions based on *HASPB18b::GFP* were amplified using 5' primers 8–11 with 3' primer 7 and cloned into *pX NEO* using *Bam*HI and *Xba*I, generating *pX NEO HASPB18::GFP*; *pX NEO haspb18 Δ Myr::GFP*; *pX NEO haspb18 Δ Palmitate::GFP*; *pX NEO haspb18 Δ Myr/Palmitate::GFP*.

Fusions encoding the first 9 or 10 amino acids of HASPB at the N terminus of EGFP were amplified from EGFP template using 3' primer 7, and 5' primers (primers 12 and 13) encoding a *Bam*HI site and the N-terminal 9 or 10 amino acids of HASPB, (CGCGGATCCATGGGAA-GCTCTTGCACGAAGGACTCCATGAGTAAAGGAGAAGAAGCTTTTC) and (CGCGGATCCATGGGAAAGCTTGTGCACGAAGGACTCCGC-

AATGAGTAAAGGAGAAGAAGCTTTTC), respectively. Fusions were cloned into *pX NEO* creating *pX NEO HASPB9::GFP* and *pX NEO HASPB10::GFP*.

pX NEO GFP was made by amplifying EGFP using 3' primer 7 and 5' primer 6 and cloning the product into the *Sma*I and *Xba*I sites of *pX NEO*.

Fusions were verified by sequence analysis using the SequenaseTM Version II Kit (United States Biochemical Corp.).

Immunoelectron Microscopy—Cells were fixed in 200 mM Pipes, 0.5 mM MgCl₂, pH 7.0, with 4% paraformaldehyde for 45 min at 4 °C. The cells were washed, pelleted in 10% gelatin in Pipes buffer, and infiltrated in 20% pyrrolidone, 1.86 M sucrose in Pipes buffer. The pellet was plunge-frozen in liquid nitrogen, and sections were cut on an MT7/CR21 cryomicrotome. Sections were placed on grids and blocked in 5% goat serum, 5% fetal calf serum in Pipes buffer (block buffer), and incubated in rabbit anti-GFP diluted 1:100 in block buffer or anti-GENE10 diluted 1:50 in block buffer. The grids were washed in block buffer and incubated in second antibody; 18 nm gold-conjugated goat anti-rabbit IgG or 12 nm gold-conjugated goat anti-mouse IgG (Jackson ImmunoResearch). Grids were washed sequentially with block buffer, Pipes buffer, and H₂O prior to embedding in 0.3% uranyl acetate in 20% methylcellulose.

***L. major* Cell Stains and Fluorescent Microscopy**—All cells were fixed by the direct addition of 3.7% formaldehyde to the culture medium and subsequently washed twice in serum-free media before spotting onto polylysine-coated multiwell slides (BDH). The flagellar pocket was visualized by incubating cells for 1 h at room temperature with tetramethylrhodamine isothiocyanate-labeled concanavalin A (Sigma) at 5 μ g/ml in serum-free medium supplemented with 1.8% de-fatted BSA. Slides were then washed twice with the BSA-supplemented serum-free medium. BODIPY TR ceramide (Molecular Probes) was used to visualize the Golgi complex. The lipid probe was conjugated with BSA by incubating 0.5 μ M in serum-free medium supplemented with 1.8% de-fatted BSA for 1 h at 4 °C. Cells were incubated for 1 h at room temperature with the conjugated probe and then back-extracted twice with serum-free medium supplemented with 1.8% de-fatted BSA (21). All cells were DNA stained with DAPI at 0.5 μ g/ml in PBS. Coverslips were mounted with Vector Shield (Vector Laboratories), and the slides were viewed using a Nikon Microphot-FX epifluorescent microscope. Images were captured with a Photometrics CH350 CCD camera coupled to a Power Macintosh G3 with the IP Lab software package (Scanalytics, Inc.) and subsequently augmented using Adobe Photoshop.

Mammalian Cell Stains and Fluorescent Microscopy—Cells were washed with PBS, fixed by the addition of 3.7% formaldehyde, and where required, permeabilized by incubating in 0.5% Triton X-100 in PBS. The cells were blocked with 10% fetal calf serum in PBS for 30 min, incubated with T7-Tag monoclonal antibody (Novagen) or anti-hGH polyclonal rabbit antibody (22) in blocking solution overnight at 4 °C, and washed 3 times. Texas Red-conjugated anti-mouse and dichlorotriazinylaminofluorescein-conjugated anti-rabbit antibodies (Jackson ImmunoResearch) were used according to the manufacturer's protocol, cells were washed 3 times, and DNA stained using 0.5 μ g/ml DAPI in PBS. After mounting in Vector Shield, the cells were observed using a Nikon Microphot-FX epifluorescent microscope and photographs taken with a Nikon FX-35DX camera. Images were scanned and manipulated using Adobe Photoshop.

Biotinylation and Fractionation of Cell Surface Proteins—Transfected *Leishmania* cell lines were gently washed 3 times and resuspended at 10⁸/ml in PBS, pH 7.4. EZ-LinkTM NHS-SS-Biotin (Pierce) was added to 1 mM and the cells incubated for 2 h at 4 °C. Cells were then gently washed 3 times in PBS, pH 7.4, 50 mM NH₄Cl and once in PBS, pH 7.4. Cells were lysed in 200 μ l of PBS, 1% SDS, boiled, and adjusted to 1 ml with PBS, 2% Triton X-100. Biotinylated proteins were then removed by incubation for 1 h at room temperature with streptavidin-agarose (Life Technologies, Inc.), separated together with the remaining unlabeled material by SDS-PAGE, then Western-blotted and probed as described.

Quenching of Surface-localized GFP Fusion Proteins—Aliquots of 10⁷ *Leishmania* were pelleted, washed, and resuspended in PBS, pH 5.0 or pH 8.0. The excitation spectra were measured using a Perkin-Elmer LS50B Luminescence Spectrometer and the FL Winlab software package, slit width at 10 nm, emission detected at 508 nm, and excitation scanned at 400–485 nm at 500 nm/min.

Membrane Fractionation—All steps were performed at 0–4 °C. 20 ml of cells at 10⁷/ml were pelleted and washed once in PBS. After resuspension in 0.5 ml of lysis buffer (0.2 M Tris, pH 8.0, 6 mM MgCl₂, 1 mM EGTA, 1 mM dithiothreitol, 100 μ g/ml phenylmethylsulfonyl fluoride, 100 μ g/ml L-1-tosylamido-2-phenylethyl chloromethyl ketone, 2 μ g/ml

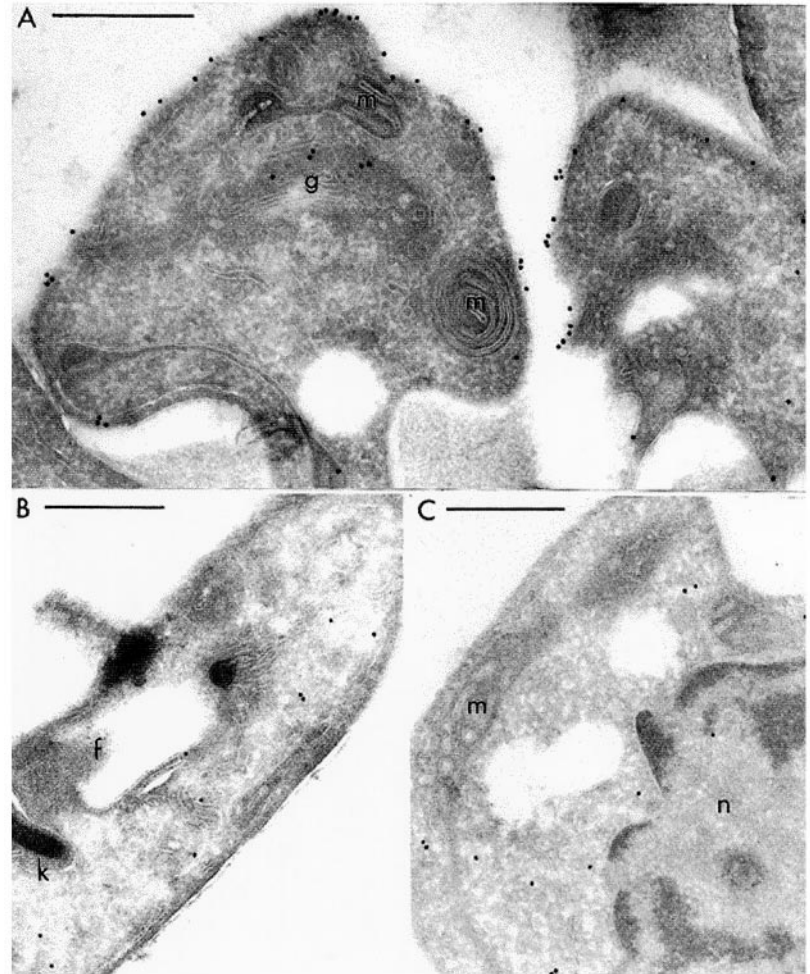
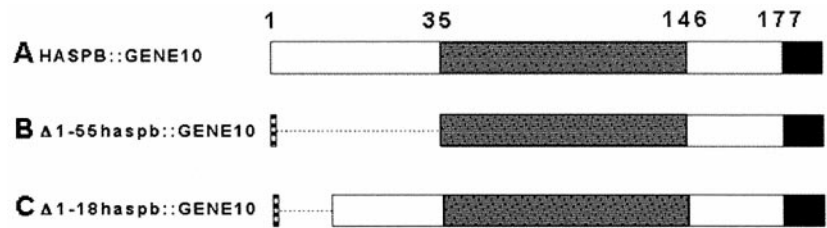


FIG. 1. Export of HASPB is mediated by its N terminus. HASPB and various deletions fused to a GENE10 tag (black box) are shown schematically with the corresponding immunoelectron micrographs of *L. major* probed with mouse anti-GENE10 antibody and 18-nm gold goat anti-mouse IgG. **A**, full-length HASPB::GENE10. The signal is localized to the periphery of the cell and in the region of the Golgi apparatus (*g*). **B**, the N-terminal 55 amino acids have been deleted. $\Delta 1-55$ haspb18::GENE10 is found in the cell cytosol. **C**, $\Delta 1-18$ haspb::GENE10, in which the N-terminal 18 amino acids have been removed, also fails to be delivered to the cell periphery. *f*, flagellum; *k*, kinetoplast; *m*, mitochondrion; *n*, nucleus. Scale bars, 0.5 μ m. N-terminal initiator methionine residues were introduced by cloning in constructs $\Delta 1-55$ haspb::GENE10 and $\Delta 1-18$ haspb::GENE10 (horizontal hatched boxes); broken lines indicate deleted regions. Shaded and non-shaded regions indicate the domains of HASPB, with amino acids numbered above construct A.

aprotinin) cells were disrupted using 300- μ m glass beads (Sigma). Undisrupted cells were cleared by a 10-min 500 $\times g$ spin, and membranes were isolated by ultra-centrifugation at 100,000 $\times g$ for 1 h in a Beckman TLA 100.3 rotor. Cytosol fractions were precipitated with 10% trichloroacetic acid for 10 min and washed in 70% ethanol.

Electrophoresis and Western Blotting—Cell or fractionation pellets were resuspended in running buffer, boiled, and separated by SDS-PAGE. Proteins were electrophoretically transferred to Immobilon P membranes (Millipore). Metabolically labeled proteins were detected using the Kodak BioMax TranScreen intensifying screen system. GFP fusion proteins were detected using the anti-GFP polyclonal antibody (CLONTECH) according to the manufacturer's instructions. GP63 was detected using a polyclonal antibody (kindly provided by Dr. Rob McMaster, University of British Columbia).

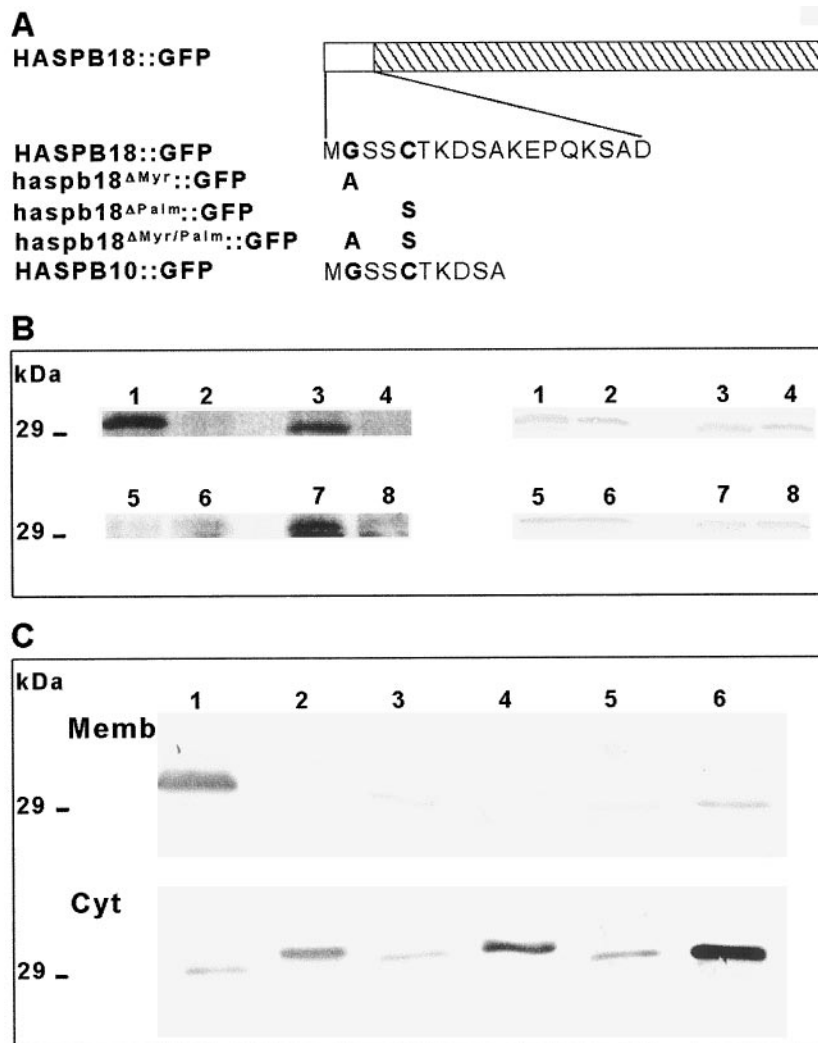
RESULTS

Deletion Mapping of the HASPB Localization Signal—The 177-amino acid *L. major* HASPB can be divided into three distinct regions (5) as follows: the N-terminal domain (amino acids 1–55), the repeat domain (amino acids 56–145), and the C-terminal domain (amino acids 146–177). By using a “deletion-fusion” approach, gene constructs were generated in which various portions of the HASPB open reading frame were fused

with a 3' GENE10 tag. Following transfection, the subcellular localization of these fusion proteins in *L. major* was established using immunoelectron microscopy. Like the wild-type protein (5, 6), full-length tagged HASPB localized to the cell periphery; in addition small quantities were detected at an internal structure identified morphologically as the Golgi (Fig. 1A). These observations confirm that the C-terminal tag does not affect HASPB localization and suggest that despite the lack of a classical secretory signal sequence, the endomembrane network is involved in transport of the protein to the cell surface. On deletion of the N-terminal 55 or 18 amino acids of HASPB, the fusion protein was localized exclusively in the cytosol (Fig. 1, B and C). The extreme N terminus of HASPB encodes a consensus for acylation by myristic acid at glycine 2 and palmitic acid at cysteine 5 (Fig. 2A). The results of these deletion experiments imply that acylation may play a role in the trafficking and attachment of the HASPB proteins to the cell surface.

HASPB Is Modified by Two Acyl Groups—To facilitate analysis of the role of the HASPB N-terminal 18 amino acids in

FIG. 2. A, HASPB18::GFP fusion proteins. The N-terminal HASPB 18 amino acids are illustrated fused to GFP (hatched box). Mutations of the glycine and cysteine residues required for myristoylation/palmitoylation and a fusion using solely the N-terminal HASPB 10 amino acids are also pictured. B, HASPB18::GFP is dually acylated. HASPB18::GFP and its mutants were labeled with ^3H -fatty-acids and detected by autoradiography (left-hand tracks) or anti-GFP antibody (right-hand tracks). 1, myristate-labeled HASPB18::GFP; 2, myristate-labeled haspb18 $\Delta^{\text{Myr/Palm}}$::GFP; 3, palmitate-labeled HASPB18::GFP; 4, palmitate-labeled haspb18 $\Delta^{\text{Myr/Palm}}$::GFP; 5, myristate-labeled haspb18 Δ^{Myr} ::GFP; 6, palmitate-labeled haspb18 Δ^{Myr} ::GFP; 7, myristate-labeled haspb18 Δ^{Palm} ::GFP; 8, palmitate-labeled haspb18 Δ^{Palm} ::GFP. C, dual acylation is required for tight membrane association. Upper panel, Memb is the membrane pellet obtained after high speed centrifugation of transfected *L. major* cell lysates. Lower panel, Cyt is the supernatant, the cytosolic fraction. Anti-GFP antibody was used to detect chimeric proteins. 1, HASPB18::GFP; 2, haspb18 Δ^{Myr} ::GFP; 3, haspb18 Δ^{Palm} ::GFP; 4, haspb18 $\Delta^{\text{Myr/Palm}}$::GFP; 5, HASPB10::GFP; 6, native GFP. The variations in protein migration size are due to changes in the length of constructs and the presence or absence of acyl groups.



transport, a series of GFP fusion constructs were made in which the HASPB consensus signals for myristoylation and palmitoylation were disrupted by site-directed mutagenesis (Fig. 2A). *L. major* parasites expressing these fusion proteins were metabolically labeled with either myristic or palmitic acids, and following separation by SDS-PAGE, radiolabeled proteins were detected by autoradiography (Fig. 2B). As expected, the HASPB18::GFP fusion protein incorporated both myristate (track 1) and palmitate (track 3) suggesting that HASPB is a dually acylated protein. The fusion protein with both putative acylation sites mutated, haspb18 $\Delta^{\text{Myr/Palm}}$::GFP, incorporated neither acyl group, confirming usage of these sites *in vivo* (tracks 2 and 4). When the myristoylation site alone was mutated, haspb18 Δ^{Myr} ::GFP, the fusion protein failed to incorporate either myristate or palmitate (tracks 5 and 6). In contrast, mutation of the palmitoylation site alone, haspb18 Δ^{Palm} ::GFP, resulted in a myristoylated but non-palmitoylated protein (tracks 7 and 8). The failure of haspb18 Δ^{Myr} ::GFP to be palmitoylated is reminiscent of the situation observed in some members of the Src family of tyrosine kinases and in several G protein α subunits, (reviewed in Ref. 23). It is probable that this is due to the inability of these mutated proteins to be co-translationally myristoylated, thus precluding association with membranes and, subsequently, with a putative membrane-bound palmitoyltransferase (23).

Membrane Association of HASPB18::GFP and Its Acyl Mutants—It has been postulated that many acylated proteins

anchor in membranes using a “two-signal” system (reviewed in Ref. 23), in which a combination of two fatty acid modifications or one fatty acid moiety and a polybasic stretch of amino acids is sufficient to tightly associate proteins with membranes. The association of HASPB18::GFP, its non-acylated mutants, and HASPB10::GFP with *L. major* membranes was assessed by fractionation and Western blotting (Fig. 2C). In the control parasites expressing native GFP, protein was predominantly found in the cytosolic fraction (track 6) as predicted, with minor contamination of the membranes. The parental fusion, HASPB18::GFP, localized solely to the membrane fraction (track 1), indicating that dual acylation is sufficient for tight membrane association. The minor fraction of smaller protein detected in the cytosolic fraction is thought to represent native GFP expressed from its own methionine start codon within the construct. The non-acylated fusion proteins, haspb18 Δ^{Myr} ::GFP and haspb18 $\Delta^{\text{Myr/Palm}}$::GFP, were detected exclusively in the cytosolic fraction (tracks 2 and 4), as would be predicted from the micrographs shown in Fig. 3. The myristoylated, non-palmitoylated fusion, haspb18 Δ^{Palm} ::GFP, was distributed equally between the membrane and cytosolic fractions (track 3). Presumably, this represents a decrease in the protein’s affinity for membranes, commensurate with the decrease in its hydrophobicity resulting from the loss of the palmitate moiety (reviewed in Ref. 24). These results provide support for the two-signal model in that both myristate and palmitate are required for stable membrane association. HASPB10::GFP (Fig. 2A) was also distributed between the membrane and

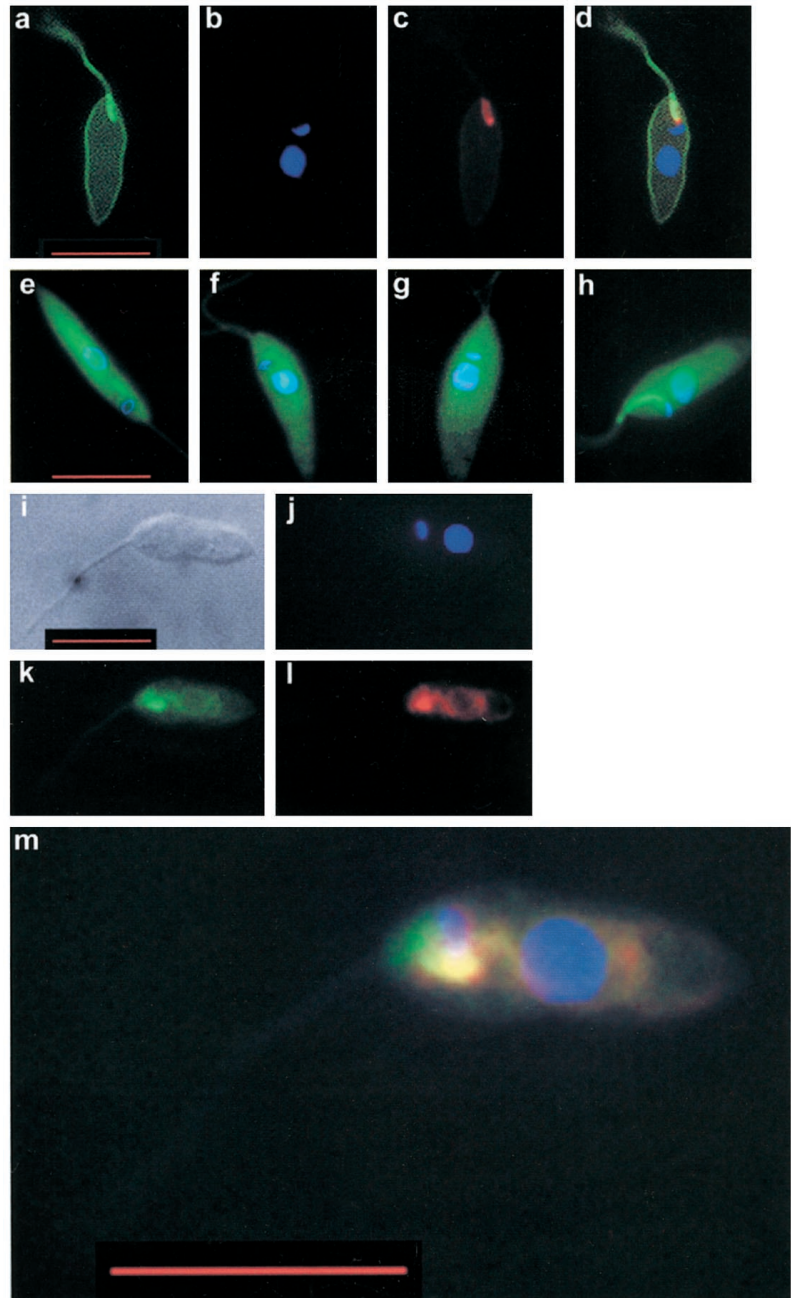


FIG. 3. Localization of HASPB18::GFP and its acyl mutants. Epifluorescent images of *L. major* expressing various GFP constructs (in green). Counterstaining is as follows: with DAPI (in blue) for the nuclear DNA and the smaller kinetoplast located near the base of the flagellum; with conA (in red) for the flagellar pocket; with BODIPY TR ceramide (in red) for the Golgi. HASPB18::GFP: *a*, GFP; *b*, DAPI; *c*, conA; *d*, overlay of *a-c*, showing co-localization at the flagellar pocket of the GFP fusion and conA. *e*, haspb18^{ΔMyr}::GFP, overlay of GFP and DAPI; *f*, haspb18^{ΔMyr/Palm}::GFP, overlay of GFP and DAPI; *g*, native GFP, overlay of GFP and DAPI; *h*, HASPB10::GFP, overlay of GFP and DAPI. haspb18^{ΔPalm}::GFP: *i*, Nomarski image; *j*, DAPI; *k*, GFP; *l*, BODIPY TR ceramide; *m*, overlay of *j-l*, showing co-localization of the Golgi maker and the GFP fusion. Scale bars, 10 μ m.

cytosolic fractions (approximately 25:75%; track 5), reflecting the partial cytosolic localization observed at a cellular level under epifluorescence (Fig. 3*h*). This chimeric protein is largely cytosolic despite maintaining the dual acylation consensus, suggesting that the acyl groups are partially inaccessible to membranes. Impaired membrane targeting of a fusion protein comprising a short, acylated signal sequence immediately proximal to GFP has been previously noted in mammalian cells (25).

The Role of Acyl Groups in Trafficking and Localization—The autofluorescent protein tag, GFP, allowed evaluation of the impact of the mutations affecting fatty acid modification on the cellular localization of HASPB18::GFP in *L. major* by epifluorescent microscopy. Tetramethylrhodamine isothiocyanate-labeled concanavalin A (conA) was used to identify the *Leishmania* flagellar pocket, the region of the plasma membrane intermediate in the trafficking of membrane-bound molecules between intracellular compartments and the cell surface (12).

Fluorophor-labeled conA has also been shown to localize to the pocket in the closely related parasites, *Trypanosoma* (26). Cells were also stained with a Golgi-specific lipid probe, BODIPY TR ceramide (Molecular Probes). The nuclear DNA and the kinetoplast were visualized using DAPI.

The parental construct, HASPB18::GFP, clearly localized to the cell periphery, including the flagellum and flagellar pocket as demonstrated by co-localization with conA and its position relative to the kinetoplast (Fig. 3, *a-d*). This is consistent with the staining pattern observed when HASP-specific antibodies were used in immunofluorescence assays with *L. major* promastigotes (5, 7). Unlike immunoelectron microscopy, epifluorescent methods have not detected HASP proteins or fusions associated with an organelle resembling the Golgi apparatus, presumably because the Golgi harbors relatively low concentrations of HASP proteins at any given time. However, the clear accumulation of protein in the flagellar pocket suggests that the HASP proteins traverse this organelle on the way to

their final destination, in a manner consistent with that proposed for trypanosomatid cell surface molecules transported by the classical mechanism (12).

The non-acylated *haspb18*^{ΔMyr/Palm}::GFP was completely localized in the cytosol (Fig. 3*f*), resembling the pattern of fluorescence observed for *Leishmania* cells expressing GFP alone (Fig. 3*g*). This demonstrates that the acyl groups are a necessary requirement for trafficking and/or localization of HASPB. The fusion protein mutated in only the myristoylation site, *haspb18*^{ΔMyr}::GFP, also showed cytosolic localization (Fig. 3*e*), consistent with metabolic labeling that demonstrated a lack of modification with myristate or palmitate (Fig. 2*B*). All three cell lines show a subcellular localization consistent with the results obtained by membrane fractionation (Fig. 2*C*).

In contrast, the *haspb18*^{ΔPalm}::GFP, shown to be myristoylated but not palmitoylated, accumulated in an organelle that also stained with the Golgi-specific probe BODIPY TR ceramide (Fig. 3, *i-m*). This indicates that the Golgi is involved in the trafficking of HASPB to the flagellar pocket and beyond. In support of this observation, immunoelectron microscopy detected small quantities of full-length GENE10-tagged HASPB in the region of the Golgi (Fig. 1*A*). The accumulation of *haspb18*^{ΔPalm}::GFP in the Golgi has been confirmed by immunoelectron microscopy (Fig. 4*C*).

A further fusion protein containing only the 10 N-terminal amino acids of HASPB, HASPB10::GFP, was made. Despite maintaining the consensus amino acids for myristoylation and palmitoylation, this protein accumulated at the flagellar pocket and also within the cytosol (Fig. 3*h*). Thus, whereas the HASPB N-terminal 10 amino acids are sufficient to localize a proportion of the fusion protein to the flagellar pocket, downstream residues appear to be required for redistribution to the cell periphery. A fusion with only the first 9 HASPB amino acids, HASPB9::GFP, was completely de-localized to the cytosol (data not shown), suggesting that this construct is either non-acylated or that the fatty acid moieties are inaccessible to membranes or otherwise non-functional.

Immunoelectron Microscopy of Cells Expressing HASPB-18::GFP—A more detailed picture of the subcellular localization of the parental construct, HASPB18::GFP, was obtained by immunoelectron microscopy. The fusion protein showed a similar pattern of localization as the full-length GENE10-tagged HASPB (compare Figs. 1*A* and 4*A*); the cell was labeled at the periphery, including the flagellum. In order to determine on which side of the plasma membrane HASPB18::GFP is located, cells were antibody-stained prior to fixation. The deposition of gold particles on the external face of the plasma membrane demonstrates that the fusion protein is exposed at the parasite surface (Fig. 4*B*), indicating that the N-terminal 18 amino acids of HASPB are sufficient for targeting and translocation of GFP to this location. Cryo-sections of the cells expressing the palmitoylation mutant *haspb18*^{ΔPalm}::GFP show protein accumulating in the region of the Golgi stacks (Fig. 4*C*). This confirms the fluorescence data shown above and indicates that like wild-type HASPB, the HASPB18::GFP fusion is exported via the endomembrane network.

Assay of GFP Surface Localization—To confirm the surface localization observed in Fig. 4*B*, the surface proteins of transfected, live cells were analyzed following biotinylation. The surface proteins of *Leishmania* expressing HASPB18::GFP and GFP were labeled with cleavable, membrane-impermeable NHS-SS-biotin and, following isolation on streptavidin-agarose, fractionated together with non-biotinylated proteins by SDS-PAGE. Fig. 5 shows that whereas GFP resides solely in the non-biotinylated fraction (compare tracks 1 and 3), HASPB18::GFP is partially biotinylated (compare tracks 2 and

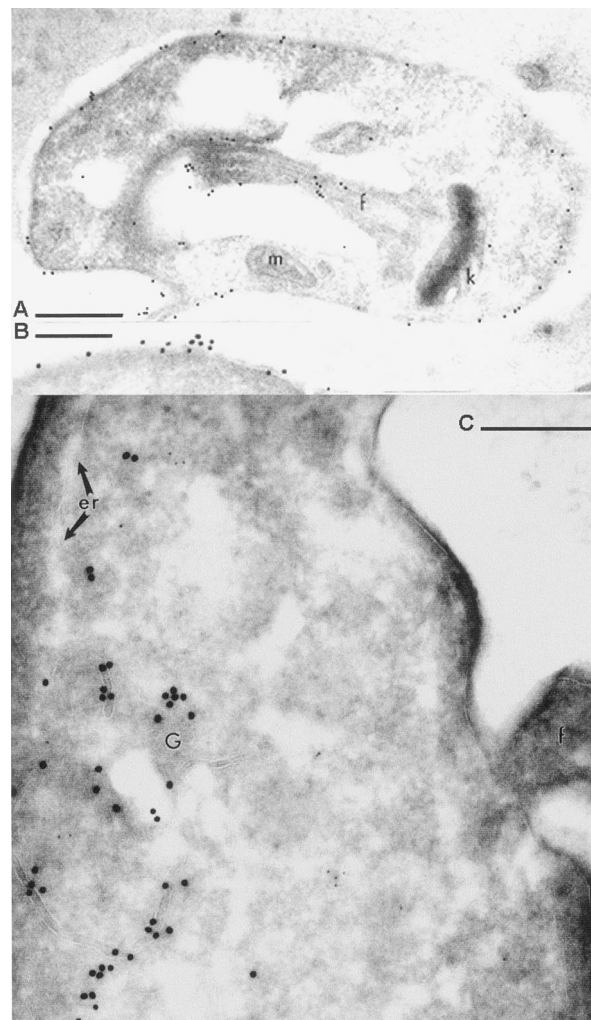


FIG. 4. Localization of HASPB18::GFP and *haspb18*^{ΔPalm}::GFP by immunoelectron microscopy. Parasites were labeled with rabbit anti-GFP antibody and 18-nm gold goat anti-rabbit IgG either pre- or postfixation and sectioning. *A*, HASPB18::GFP labeled after fixation and sectioning. The gold label is seen on the plasma membrane that covers the cell body and the flagellum. Scale bar, 0.5 μ m. *B*, HASPB18::GFP labeled prior to fixation and sectioning. The label can be seen on the cell surface demonstrating that at least a portion of the HASPB18::GFP fusion protein is surface-exposed. Controls conducted on wild-type *L. major* were negative for gold labeling. Scale bar, 0.25 μ m. *C*, *haspb18*^{ΔPalm}::GFP localized to the Golgi stacks. Scale bar, 0.25 μ m. *er*, endoplasmic reticulum; *f*, flagellum; *G*, Golgi; *k*, kinetoplast; *m*, mitochondrion.

4). This indicates that a proportion of HASPB18::GFP, estimated at 30% by densitometry, is accessible to biotin. The major surface glycoprotein GP63 is detected solely within the biotinylated fraction as would be expected (compare tracks 5 and 6).

To confirm further the orientation of HASPB18::GFP at the plasma membrane, a novel live cell assay was developed based on the observation that the fluorescence of GFP and its variants decreases at reduced pH (27). *L. major* parasites expressing HASPB18::GFP, *haspb18*^{ΔMyr/Palm}::GFP, or GFP alone were washed and resuspended in PBS adjusted to pH 5.0 or 8.0, and fluorescence emission was measured at 508 nm (see under "Experimental Procedures").

The emission of cells expressing GFP were unchanged at reduced pH (Table I), consistent with the molecule being cytosolic and unexposed to the extracellular environment, and demonstrating that under these conditions the *Leishmania* cytosol remains buffered at a neutral pH. Similarly, parasites express-

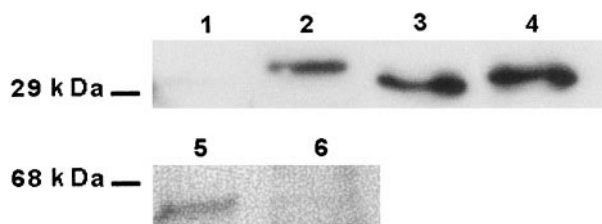


FIG. 5. **Surface biotinylation HASPB18::GFP.** *L. major* expressing soluble GFP (tracks 1 and 3) or HASPB18::GFP (tracks 2 and 4–6) were biotinylated using a membrane-impermeable biotin reagent and labeled proteins (tracks 1, 2, and 5) separated from unlabeled material (tracks 3, 4, and 6). Tracks 1–4 were immunoblotted with anti-GFP antibody; GFP was undetectable in the biotinylated fraction (track 1) compared with the unlabeled portion (track 3). In contrast HASPB18::GFP was found to be biotinylated to significant levels, approximately 30% of total protein (compare tracks 2 and 4). The apparent difference in the molecular weight of labeled and unlabeled HASPB18::GFP could be due to modification with biotin or non-uniformity of the gel. By immunoblotting with anti-GP63 (tracks 5 and 6), the major *Leishmania* surface protein was detected predominantly in the biotinylated fraction.

ing haspb18^{ΔMyr/Palm}::GFP were unaffected by a reduction in the extracellular pH consistent with a cytosolic localization for the chimeric protein (Table I). Permeabilization of the cells with 0.1% Triton X-100 led to a dramatic loss of fluorescence at pH 5.0 but not at pH 8.0. This demonstrated that the fluorescence of HASPB-GFP fusions was pH-sensitive, as expected, and confirmed that the lack of shift is due to protection by Triton X-100-soluble structures.

In contrast to the above, the emission measured from intact parasites expressing HASPB18::GFP showed a marked decrease in fluorescence intensity at pH 5.0 (Table I), consistent with the fusion protein being surface-exposed and therefore subject to changes in environmental pH. The reduction in fluorescence was relatively small when compared with that observed after detergent disruption (Table I), suggesting that the chromophore is only partly exposed to the pH shift. By comparison with Triton X-100-treated cells, it appears that approximately 20% of HASPB18::GFP was susceptible to a reduction in pH.

Both the biotin and fluorescence assays suggest that only a proportion of HASPB is accessible to external reagents. This can be interpreted in at least two ways, either that only a minority of HASPB is presented on the extracellular face of the plasma membrane or that the surface properties of the *Leishmania* membrane prevent full penetrance of protons or biotin. *Leishmania* possess a thick, glycoconjugate-rich coat that confers a negative charge at the cell surface perhaps buffering against environmental changes (in pH for example) and repelling charged molecules such as biotin and its derivatives.

The Trafficking of HASPB in Mammalian Cells—To investigate whether the signal for export of HASPB to the cell surface of *L. major* is functional in higher eukaryotes, the full-length *GENE10*-tagged *HASPB*, *HASPB::GENE10* (cloned into a mammalian expression vector), was transfected into CHO cells stably expressing human growth hormone fusions (28) localizing either to the ER (hD28) or to the cell surface (hD29). Localization of the chimeric proteins was established in these cells by indirect immunofluorescence using monoclonal anti-*GENE10* tag and polyclonal anti-hGH antibodies (Fig. 6).

In permeabilized CHO cells, hGHDAF29 localized to the cell periphery, whereas hGHDAF28 was found in a juxtannuclear position consistent with an ER localization (28). The distribution of *HASPB::GENE10* appeared coincident with that of hGHDAF29, indicative of cell surface expression (29).

Staining of non-permeabilized CHO cells showed hGH-

DAF29 at the periphery of the cell, demonstrating that it was surface-exposed as would be expected of a protein with a secretory signal sequence and a GPI-anchor consensus motif. In contrast, hGHDAF28 was undetectable, consistent with intracellular localization (28). *HASPB::GENE10* was also detected on non-permeabilized cells confirming its location on the surface. These data demonstrate that *HASPB* can be exported to the cell surface in higher eukaryotes and suggest that the non-classical pathway observed in *Leishmania* is conserved in mammalian cells.

DISCUSSION

In the absence of a secretory signal sequence, a GPI-anchor consensus, or transmembrane domain, the pathway and mechanisms that facilitate localization of the *HASP* family proteins to the *Leishmania* cell surface have been unknown to date. Here, a deletion strategy has identified the extreme N terminus of *HASPB* as being essential for surface presentation of the protein. The presence of *N*-myristoylation and palmitoylation motifs within these residues indicates that dual acylation may mediate membrane association and also potentially act as the cell surface anchor for *HASPB*.

Two Signals Are Required for Plasma Membrane Targeting—Metabolic labeling indicated that glycine 2 and cysteine 5 in the *HASPB* N-terminal region are required for myristoylation and palmitoylation. Co-translational myristoylation is required for post-translational palmitoylation to occur, in agreement with the hypothesis that a myristate moiety is required to bring the protein to a membrane-bound palmitoyltransferase (23). According to the two-signal model (23), such modifications would be sufficient to allow the stable association of *HASPB* with membranes previously observed (5, 6). Many proteins have been shown to be targeted to the plasma membrane by dual acylation. The mechanism of targeting is unclear, although the identification of a $G\alpha$ protein palmitoyltransferase activity in plasma membrane fractions (30) supports a model in which an *N*-myristoylated protein could become “trapped” in a lipid bilayer when it associates with this putative enzyme and is palmitoylated (Refs. 31 and 32 and references therein).

The requirement of dual acylation for stable membrane association and targeting to the plasma membrane was tested using a series of fusion proteins expressed in *L. major*, in which the N-terminal *HASPB* 18 amino acids were fused to the N terminus of GFP. Cell fractionation demonstrated that both myristate and palmitate were necessary for efficient membrane binding; myristate alone led to only partial association. Epifluorescent microscopic analyses were consistent with these observations, as the fusion protein required both myristoylation and palmitoylation signals to facilitate localization to the plasma membrane.

Trafficking of *HASP* through the Cell—The route dually acylated proteins take to the plasma membrane has only recently been investigated. Trafficking of the *N*-myristoylated/palmitoylated Src tyrosine kinase, Fyn, to the plasma membrane in mammalian cells is thought to occur very rapidly via a novel pathway (31). Another dually acylated Src protein, Lck, was found at the plasma membrane and in the Golgi by co-localization when expressed in certain mammalian cell lines (33). These observations implicate the Golgi apparatus in Lck trafficking. Immunoelectron microscopy of *L. major* expressing full-length *GENE10*-tagged *HASPB* or the parental GFP construct, *HASPB18::GFP*, revealed the protein localizing primarily to the plasma membrane but with some Golgi-associated staining (only detectable by this highly sensitive method). Such data support an hypothesis in which the Golgi and by extrapolation the exocytic pathway are involved in both Src and

TABLE I
Effect of pH on the relative fluorescence intensity of *Leishmania* expressing different GFP constructs

| Construct | Triton X-100 | Relative fluorescence intensity (\pm S.D.) | | Significance ^a ($p <$) |
|--------------------------------|--------------|---|----------------|-------------------------------------|
| | | pH 8.0 | pH 5.0 | |
| GFP | – | 100 \pm 3.8 | 104 \pm 6.2 | NS |
| haspb18 Δ Myr/Palm::GFP | – | 100 \pm 1.2 | 99.7 \pm 0.3 | NS |
| haspb18 Δ Myr/Palm::GFP | + | 100 \pm 2.9 | 21 \pm 0.1 | 0.0001 ^b |
| HASPB18::GFP | – | 100 \pm 0.9 | 85.1 \pm 4.2 | 0.004 ^c |
| HASPB18::GFP | + | 100 \pm 2.1 | 17.3 \pm 0.7 | 0.0001 ^b |

^a Student's unpaired *t* test performed to establish significance (*p*) of the difference in fluorescence intensity observed in cells at pH 8.0 and pH 5.0. The difference is non-significant (NS) for cytosolic GFP and haspb18 Δ Myr/Palm::GFP, unless the cells are disrupted with Triton X-100. Parasites expressing HASPB18::GFP show highly significant reduction in fluorescence intensity at pH 5.0 with Triton X-100 but also significant at pH 5.0 in the absence of detergent, indicating the presence of the chimeric protein on the cell surface. Data were taken in triplicate from two independent experiments, standardized to 100% and S.D. calculated.

^b highly significant.

^c significant.

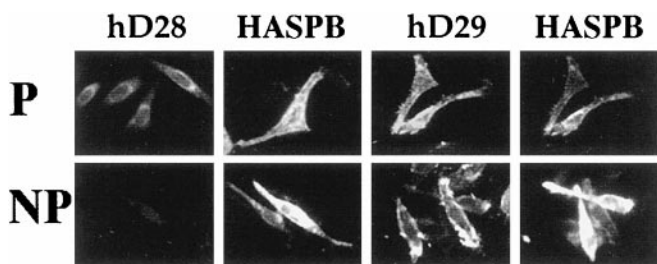


FIG. 6. **The HASPB export pathway is conserved in higher eukaryotes.** Immunofluorescence assays of CHO cells co-expressing HASPB::GENE10 with the ER marker hD28 or the plasma membrane marker hD29. Cells were either permeabilized (*P*) or non-permeabilized (*NP*) prior to immunodetection. Unlike the internal ER marker hD28, hD29 and HASPB::GENE10 were detected at the cell surface in non-permeabilized cells.

HASP trafficking. Another particularly striking observation is that mutation of the HASP palmitoylation site in this chimera leads to the protein concentrating in an organelle stained by a Golgi-specific lipid marker. This supports the suggestion that palmitoylation of *N*-myristoylated proteins occurs at a membranous structure possibly belonging to the exocytic pathway (33). This situation is reminiscent of the trafficking of certain acylated Ras proteins that have recently been suggested to be targeted to the endomembrane network (including the Golgi) by virtue of prenylation. Further trafficking of these proteins to the plasma membrane is dependent upon subsequent palmitoylation (34).

Therefore, this study implicates the exocytic structures in the transport of HASP, despite the lack of an ER secretory signal. In addition, like other dually acylated proteins (31), the trafficking of HASPB in a mammalian system was unaffected by brefeldin A, a potent inhibitor of anterograde vesicular transport (data not shown). Our data, like that of Bijlmakers *et al.* (33), imply that palmitoylation occurs in the region of the Golgi, with subsequent re-localization to the plasma membrane. This contrasts with the proposal that Fyn is targeted directly to and palmitoylated at the plasma membrane (31). However, van't Hof and Resh (31) detected a small quantity of Fyn in Golgi membrane fractions. This fraction could be analogous to the HASPB detected in the region of the Golgi apparatus and could explain the partial perinuclear localization of Fyn (31).

Recently, several studies have suggested that proteins modified by saturated acyl groups are targeted to detergent-resistant membrane (DRM) rafts in mammalian cells (35). These DRMs are implicated in protein sorting in the secretory pathway (36). In keeping with our trafficking model, it may be predicted that *N*-myristoylated/palmitoylated proteins associate with DRMs on the cytoplasmic face of structures in the exocytic pathway and are subsequently transported to the

plasma membrane. It is possible that any other machinery required for localization is brought to its protein target by association with these rafts. In the case of HASP, this machinery may include a palmitoyltransferase and some translocation channel, such as that discussed below, to allow the protein to reach the extracellular environment.

HASP Appears to Be Localized to the Cell Surface by a Conserved, Novel Pathway—Despite incomplete characterization of the mechanism, it is clear that *N*-myristoylation/palmitoylation is sufficient to traffic a large number of proteins to the plasma membrane (32). Unlike these other examples, HASPB is surface-localized in *L. major* (5, 6) despite lacking any identifiable signal that could lead to translocation by the exocytic pathway. Electron microscopic and biochemical analyses demonstrate that the N-terminal 18 amino acids of HASPB are sufficient to take a heterologous protein (GFP) to the cell surface. Whereas *N*-myristoylation/palmitoylation is presumably sufficient to transport HASPB to the cytoplasmic face of the plasma membrane, some additional determinant within the 18-amino acid signal is presumed to facilitate translocation of a proportion of the protein across the membrane and into the extracellular environment. The N-terminal 10 amino acids of HASPB, maintaining the acylation consensus, are sufficient only to take GFP as far as the flagellar pocket. The reasons for biochemically detecting only 20–30% of HASPB18::GFP at the cell surface are unclear and, as discussed above, could be due to either limited surface presentation of the protein or limits inherent within the assays developed.

The mechanism that would take a lipid-anchored protein from one face of the plasma membrane to the other is unclear. However, one hypothesis that would fit our data is the “flip-pase” model (37) in which a membrane-bound transporter protein allows translocation of the hydrophobic anchor through the lipid phase and the relatively hydrophilic polypeptide through an aqueous channel. Recent structural evidence indicates that such a model holds true for the P-glycoprotein family of transport molecules (38). Currently knowledge of the involvement of these proteins in the secretion of eukaryotic polypeptides is restricted to export of the yeast α -mating factor (15). A genetic complementation strategy may identify molecules involved in the transport of HASPB to the cell surface.

Whatever the mechanisms involved, the targeting and translocation of the protozoan protein, HASPB, onto the surface of the plasma membrane is of general interest as it is conserved in higher eukaryotic cells. This suggests that HASPB may represent the first in a family of non-classically exported, lipid-anchored surface proteins.

Acknowledgments—We thank Drs. Paul McKean and Jane Keen for helpful discussions and critical reading of the manuscript and Dr. John Tippins for assistance with statistical analyses.

REFERENCES

1. Molyneux, D., and Killick-Kendrick, R. (1987) in *The Leishmaniasis in Biology and Medicine* (Peters, W., and Killick-Kendrick, R., eds) Vol. 1, pp. 122–168, Academic Press, London
2. Ferguson, M. A., Brimacombe, J. S., Cottaz, S., Field, R. A., Guther, L. S., Homans, S. W., McConville, M. J., Mehlert, A., Milne, K. G., Ralton, J. E., Roy, Y. A., Schneider, P., and Zitzmann, N. (1994) *Parasitology* **108**, S45–S54
3. McConville, M. J., and Ferguson, M. A. J. (1993) *Biochem. J.* **294**, 305–324
4. Frommel, T. O., Button, L. L., Fujikura, Y., and McMaster, W. R. (1990) *Mol. Biochem. Parasitol.* **38**, 25–32
5. Flinn, H. M., Rangarajan, D., and Smith, D. F. (1994) *Mol. Biochem. Parasitol.* **65**, 259–270
6. Pimenta, P. F. P., Da Silva, P. P., Rangarajan, D., Smith, D. F., and Sacks, D. L. (1994) *Exp. Parasitol.* **79**, 468–479
7. Rangarajan, D., Gokool, S., McCrossan, M. V., and Smith, D. F. (1995) *J. Cell Sci.* **108**, 3359–3366
8. Clayton, C., Hausler, T., and Blattner, J. (1995) *Microbiol. Rev.* **59**, 325–344
9. Al-Qahtani, A., Teilhet, M., and Mensa-Wilmot, K. (1998) *Biochem. J.* **331**, 521–529
10. Tobin, J. F., and Wirth, D. F. (1993) *Mol. Biochem. Parasitol.* **62**, 243–248
11. Webster, P., and Russell, D. G. (1993) *Parasitol. Today* **9**, 201–205
12. Overath, P., Stierhof, Y.-D., and Wiese, M. (1997) *Trends Cell Biol.* **7**, 27–33
13. Kuchler, K. (1993) *Trends Cell Biol.* **3**, 421–426
14. Cleves, A. E. (1997) *Curr. Biol.* **7**, R318–R320
15. Kuchler, K., Sterne, R. E., and Thorner, J. (1989) *EMBO J.* **8**, 3973–3984
16. Mehul, B., and Hughes, R. C. (1997) *J. Cell Sci.* **110**, 1169–1178
17. Cleves, A. E., Cooper, D. N. W., Barondes, S. H., and Kelly, R. B. (1996) *J. Cell Biol.* **5**, 1017–1026
18. LeBowitz, J. H., Coburn, C. M., McMahon-Pratt, D., and Beverley, S. M. (1990) *Proc. Natl. Acad. Sci. U. S. A.* **87**, 9736–9740
19. Field, M. C., and Menon, A. K. (1992) in *Lipid Modification of Protein* (Hooper, N. M., and Turner, A. J., eds) pp. 155–190, Oxford University Press, Oxford
20. Cormack, B. P., Valdivia, R., and Falkow, S. (1996) *Gene (Amst.)* **173**, 33–38
21. Pagano, R. E., Sepanski, M. A., and Martin, O. C. (1989) *J. Cell Biol.* **109**, 2067–2079
22. Wainwright, L. J., and Field, M. C. (1997) *Biochem. J.* **321**, 655–664
23. Resh, M. D. (1996) *Cell. Signal.* **8**, 403–412
24. Bhatnagar, R. S., and Gordon, J. I. (1997) *Trends Cell Biol.* **7**, 14–20
25. Fraser, I. D. C., Tavalin, S. J., Lester, L. B., Langeberg, L. K., Westphal, A. M., Dean, R. A., Marrior, N. V., and Scott, J. D. (1998) *EMBO J.* **17**, 2261–2272
26. Balber, A. E., and Frommel, T. O. (1988) *J. Protozool.* **35**, 214–219
27. Bokman, S. H., and Ward, W. W. (1981) *Biochem. Biophys. Res. Commun.* **101**, 1372–1380
28. Field, M. C., Moran, P., Li, W., Keller, G. A., and Caras, I. W. (1994) *J. Biol. Chem.* **269**, 10830–10837
29. Moran, P., and Caras, I. W. (1992) *J. Cell Biol.* **119**, 763–772
30. Dunphy, J. T., Greentree, W. K., Manahan, C. L., and Linder, M. E. (1996) *J. Biol. Chem.* **271**, 7154–7159
31. van't Hof, W., and Resh, M. (1997) *J. Cell Biol.* **136**, 1023–1035
32. Morales, J., Fishburn, C. S., Wilson, P. T., and Bourne, H. R. (1998) *Mol. Biol. Cell* **9**, 1–14
33. Bijlmakers, M.-J. J. E., Isobe-Nakamura, M., Ruddock, L. J., and Marsh, M. (1997) *J. Cell Biol.* **137**, 1029–1040
34. Choy, E., Chiu, V. K., Silletti, J., Feoktistov, M., Morimoto, T., Michaelson, D., Ivanov, I. E., Philips, M. R. (1999) *Cell* **98**, 69–80
35. Melkonian, K. A., Ostermeyer, A. G., Chen, J. Z., Roth, M. G., and Brown, D. A. (1999) *J. Biol. Chem.* **274**, 3910–3917
36. Simons, K., and Ikonian, E. (1997) *Nature* **387**, 569–572
37. Higgins, C. F., and Gottesman, M. M. (1992) *Trends Biochem. Sci.* **17**, 18–21
38. Rosenberg, M. F., Callaghan, R., Ford, R. F., and Higgins, C. F. (1997) *J. Biol. Chem.* **272**, 10685–10694